Discover Oncology

RESEARCH Open Access

Hypomethylation of *FAM83A* in lung adenocarcinoma mirrors an epigenetic signature of airway cell differentiation states

Camille Wangermez[1], Francois M. Carlier[1,2], Marylène Lecocq[2], Charles Pilette[2] and Charles De Smet[1*]

*Correspondence:
Charles De Smet
charles.desmet@uclouvain.be
[1]Group of Genetics and Epigenetics (GEPI), de Duve Institute, Université Catholique de Louvain, Brussels, Belgium
[2]Pole of Lung, Nose and Skin Research (LUNS), Institute of Experimental and Clinical Research (IREC), Université Catholique de Louvain, Brussels, Belgium

Abstract

DNA hypomethylation represents the most prevalent epigenetic alteration in human cancer, yet its cellular origins remain incompletely understood. In lung adenocarcinoma (LUAD), DNA hypomethylation is associated with upregulation of distinct gene groups, including: cancer-germline (CG) genes normally restricted to testicular germ cells, and stratified epithelium (SE) genes typically expressed in multilayered epithelia. Among the latter, *FAM83A* has emerged as a pro-tumoral gene implicated in cancer progression and therapy resistance. Here, we asked whether *FAM83A* activation in LUAD represents an epigenetic abnormality or if it reflects redirection of malignant cells towards an existing epithelial program. By analyzing single-cell RNA sequencing data from normal lung we found that, while *FAM83A* is undetectable in whole lung tissue homogenates, it is expressed in subsets of airway epithelial cells corresponding to basal/suprabasal and goblet cell populations. In contrast, CG gene *MAGEA1* is silent in all lung cell types. Consistently, RT-qPCR detected *FAM83A*, but not *MAGEA1*, in primary and immortalized human lung basal cells. Bisulfite sequencing showed that the promoter of *FAM83A,* but not *MAGEA1,* is unmethylated in these cells. Analyses of transcriptomic datasets from LUAD cell lines and tissues demonstrated that *FAM83A* expression is correlated with markers of suprabasal and goblet lineages in malignant cells. They further revealed co-expression of *FAM83A* with *NAPSA*, a marker of alveolar AT2 cells, from which LUAD originates. Together, these findings indicate that, whereas *MAGEA1* activation in LUAD results from an aberrant process of DNA demethylation, *FAM83A* upregulation in LUAD reflects redirection of alveolar cells towards an airway differentiation program.

1 Introduction

In many organisms, including humans, methylation of CpG dinucleotides in the DNA represents an epigenetic mechanism of long-term transcriptional gene repression [1]. During development, distinct patterns of DNA methylation are acquired by the different cell lineages, contributing to the establishment of cell-type-specific gene expression programs [2, 3]. Although some DNA methylation marks show age-related variations, most of them are faithfully preserved throughout adult life [4, 5]. In tumor cells however,

profound alterations of DNA methylation patterns are observed, including gains (hypermethylation) and losses (hypomethylation) in different parts of the genome [6]. DNA hypermethylation in tumors was shown to lead to the irreversible silencing of tumor suppressor genes, whereas DNA hypomethylation was associated with the aberrant activation of genes with tumor promoting properties [7, 8]. The latter include primarily a group of genes, including *MAGEA1*, which were collectively referred to as "Cancer-Germline" (CG), because their expression in healthy individuals is limited to testicular germ cells [9].

In a recent study investigating methylomic and transcriptomic datasets of lung adenocarcinoma (LUAD), DNA hypomethylation in cancer was found to correlate with transcriptional activation of not only CG genes, but also of another cluster of tissue-specific genes showing restricted expression in tissues that comprise a stratified squamous epithelium (skin, esophagus and vagina) [10]. Among this so-called "Stratified-Epithelium" (SE) gene cluster, *FAM83A* showed the highest frequency of upregulated expression in LUAD samples, and its expression correlated with reduced survival of the cancer patients [10]. Over the last 10 years, *FAM83A* has attracted growing interest as a tumor-promoting gene [11]. Studies in various cancer cell types have demonstrated that overexpression of FAM83A induces increased proliferation, acquisition of stem cell-like traits, and loss of cell polarity [12–14], by modulating oncogenic signaling cascades, such as the PI3K/AKT, MAPK, and Wnt/β-catenin pathways [15–17].

The origin of DNA hypomethylation in tumor cell genomes remains poorly understood. It may arise through dysregulation of the DNA methylation machinery in cancer cells, for instance as a consequence of altered expression or mutations affecting DNA methyltransferases (DNMT1, DNMT3A/B) [18–23]. Alternatively, it may be inherent to the high plasticity of cancer cells, which alter their differentiation trajectory, reshaping DNA methylation patterns to adapt gene expression programs [24, 25]. It has also been suggested that DNA hypomethylation may reflect the expansion of a pre-existing unmethylated state that was present in a discrete population of normal cells from which the tumor originated [26]. For LUAD, lineage tracing in genetically modified mouse models have identified lung alveolar type 2 (AT2) cells as the cell of origin [27, 28], and previous results showed that CG genes (e.g. *MAGEA1*) and SE genes (e.g. *FAM83A*) are repressed and methylated in these cells [10].

The advent of single-cell RNA-Seq has revealed that numerous tissue-specific transcripts are detectable only at single-cell resolution, as bulk tissue profiling averages expression across diverse cell types and thereby masks signals from rare cell populations [29]. We therefore decided to re-assess the expression and promoter DNA methylation of SE gene *FAM83A* and CG gene *MAGEA1* in normal lung cells by exploring single-cell transcriptomic data, and by performing bisulfite sequencing on airway cell cultures. We found that *FAM83A*, but not *MAGEA1*, is expressed and unmethylated in a discrete subset of lung cells that are distinct of AT2 cells. We therefore further investigated co-expression of *FAM83A* with specific markers of these lung cell types in LUAD.

2 Material and methods

2.1 Cell culture

The human bronchial epithelial cell line HBEC3-KT (CRL-4051, ATCC, Manassas, VA, USA) was cultured in Airway Epithelial Cell Basal Medium (PCS-300-030, ATCC,

Manassas, VA, USA) supplemented with the Bronchial Epithelial Cell Growth Kit (PCS-300-040, ATCC, Manassas, VA, USA). The immortalized foreskin fibroblast cell line HFF2-hTERT (kindly provided by Dr Decottignies, de Duve Institute, UCLouvain) was maintained in Dulbecco's Modified Eagle Medium (DMEM, Gibco, Thermo Fisher Scientific, Waltham, MA, USA) supplemented with 10% fetal bovine serum (FBS, Sigma-Aldrich, St-Louis, MO, USA) and 1% penicillin–streptomycin (Life Technologies, Carlsbad, CA, USA). For passaging and harvesting, HBEC3KT and HFF2-hTERT cells were detached using 0.05% trypsin–EDTA (Gibco, Thermo Fisher Scientific, Waltham, MA, USA). The derivation and ex vivo 2D culture of HBEC cells were described previously [30].

2.2 5-azadC and siRNA treatments

For 5-aza-2'-deoxycytidine (5-azadC) treatments, HFF2-hTERT cells were grown to 60–70% confluency and treated with a single dose of 2 µM 5-azadC (dissolved in 1:1 acetic acid:water). Cells were maintained in culture for 3 days before RNA extraction and RT-qPCR analyses.

For siRNA treatments, HBEC3-KT cells were seeded at 400,000 cells per well in 6-well plates and reverse-transfected with siRNAs targeting *FAM83A* (siFAM83A) or control siRNAs targeting luciferase (siLuc) at a final concentration of 100 nM, using Lipofectamine 2000 (Invitrogen, Carlsbad, CA, USA). Cells were harvested 3 days post-transfection for RNA and protein analysis. siRNA sequences were designed based on previous studies [13, 31].

2.3 RNA extraction, reverse transcription, and quantitative PCR (qPCR)

Total RNA of cell lines and frozen HBEC samples was extracted using TriPure Isolation Reagent (Sigma-Aldrich, St-Louis, MO, USA) according to the manufacturer's instructions. RNA from normal tissue samples (lung and testis) was purchased from Ambion (Thermo Fisher Scientific, Waltham, MA, USA). Reverse transcription was performed using the MML-V reverse transcriptase kit (Thermo Fisher Scientific, Waltham, MA, USA) using random hexamers (Invitrogen, Carlsbad, CA, USA), Ribolock RNAse inhibitor (20 U, Invitrogen, Carlsbad, CA, USA), and 2 µg of total RNA per reaction, in a final volume of 20 µL. qPCR analyses were carried out using the KAPA SYBR FAST kit (Sigma-Aldrich, St-Louis, MO, USA) with 1/40 of the reverse transcription product used per reaction, in a final volume of 10 µL. All reactions were performed according to the manufacturer's instructions. Primer sequences are provided in supplementary Table S1.

2.4 Western blot

At day 3 post-transfection, HBEC3-KT cells were harvested for protein extraction. Cells were lysed in RIPA buffer (150 mM NaCl, 1% TritonX-100, 0.5% sodium deoxycholate, 0.1% SDS and 50 mM Tris pH 8) supplemented with cOmplete Mini protease inhibitor cocktail (Roche, Basel, Switzerland) and PhosSTOP phosphatase inhibitor cocktail (Roche, Basel, Switzerland). Protein lysates (20 µg) were separated on 8% SDS-PAGE gels and transferred onto PVDF membranes (Millipore, Burlington, MA, USA) at 240 mA for 2 h. Membranes were blocked in 5% milk in TBS-Tween 0.1% for 1 h at room temperature (RT), then incubated for 1 h at RT with anti-FAM83A antibody (1:600, 20618-AP, Proteintech, Rosemont, IL, USA, diluted in blocking solution). After three washes in

TBS-Tween 0.1%, membranes were incubated for 1 h at RT with a goat anti-rabbit HRP-conjugated secondary antibody (1:10,000, ADI-SAB-300 J, Enzo Life Sciences, Farmingdale, NY, USA, diluted in TBS-Tween 0.1%). Signal was detected using SuperSignal West Pico PLUS Chemiluminescent substrate (Thermo Fisher Scientific, Waltham, MA, USA) and visualized with the Amersham ImageQuant 800 system (Cytiva, Marlborough, MA, USA). For Vinculin detection, membranes were stripped with 0.4 M NaOH (4 × washes), re-blocked for 1 h in 5% milk in TBS-Tween 0.1% and incubated with anti-vinculin antibody (1:100,000, 05-386, Millipore, Burlington, MA, USA) for 1 h at RT. A goat anti-mouse HRP-conjugated secondary antibody (1:10,000, ab205719, Abcam, Cambridge, UK, diluted in TBS-Tween 0.1%) was used for detection as above.

2.5 Sodium bisulfite sequencing

Sodium bisulfite genomic sequencing of the *FAM83A* and *MAGEA1* promoter regions was performed as previously described [32]. Primers used for nested PCR amplification of bisulfite-treated DNA are listed in supplementary Table S2.

2.6 DNA methylation public dataset

Whole genome bisulfite-seq (WGBS) data from normal keratinocytes, spermatozoa, the IMR90 fibroblast cell line, human embryonic stem cells (hESCs), and hESC-derived ectoderm, mesoderm, and endoderm cells were visualized using the NIH Roadmap epigenomics track viewer [33]. For quantification of CpG methylation levels in *FAM83A* 5'-region, WGBS data of keratinocytes and primary AT2 cell were obtained and processed as previously described [10]. To assess DNA methylation differences in LUAD, methylation data from the Cancer Genome Atlas (TCGA) were analyzed using the Wanderer web tool (http://maplab.imppc.org/wanderer/) [34]. CpG β-values located within the *FAM83A* regulatory region (chr8:124193000-124196000, GRCh37/hg19) were extracted and visualized. Differential methylation between normal lung and LUAD samples was evaluated using a t-test with adjusted p-values. Pearson correlations analyses were performed to assess the relationship between *FAM83A* expression and CpG methylation levels.

2.7 RNA-Seq public dataset

Bulk RNA-Seq. Expression graphs for the gene of interest in normal tissues (GTEx data) were retrieved from the Human Protein Atlas (proteinatlas.org) [35]. Correlation analyses were performed using the GEPIA2 web server (http://gepia2.cancer-pku.cn) on RNA-seq data from LUAD tumor samples (TCGA) [36], applying Spearman correlation coefficients. Correlation analyses were also performed using the DepMap portal (https://depmap.org/explorer) on RNA-seq data from LUAD cell lines [37], using Spearman correlation coefficient.

scRNA-Seq. Data from Guo et al. [41] were visualized using the ShinyCell Human Lung CellRef v1.1 (https://app.lungmap.net/app/shinycell-human-lung-cellref) [38]. UMAP visualization was generated for *FAM83A*. For epithelial cell type analysis, heatmaps were generated. Using the CellxGene platform, the percentage of epithelial cells expressing the genes of interest was calculated based on the number of total cells and the number of cells with expressing values above $\ln(\mathrm{CPTT}+1) > 1$. Data from Salcher et al. [39] were downloaded via CellxGene (https://datasets.cellxgene.cziscience.com/c1870f1f-ca36-4d

96-b03b-7dc0e96d83ee.h5ad) and analyzed in R (version 4.3.1) [39]. Only lung adenocarcinoma and cells annotated as malignant were retained for downstream analyses. Malignant cells were grouped by tumor sample (N = 108 LUAD tissues). Tumors containing fewer than 30 malignant cells were excluded. After filtering, 81 LUAD tissues were retained. Cells were considered positive for the expression of a gene when its log normalized transcription value was > 0.

2.8 Statistical analysis

Before analysis, qPCR data were tested for normality using the Shapiro–wilk test. When all groups followed a normal distribution, parametric paired t-tests were used. Data were analyzed with GraphPad Prism Version 10.5.0 for Windows (GraphPad Software). P-values < 0.05 were considered statistically significant.

3 Results

3.1 SE genes, including *FAM83A*, but not CG genes are expressed in a subgroup of lung cells

Previous RT-qPCR and RNA-Seq analyses did not detect expression of SE and CG genes in normal lung tissue samples [10]. This is further illustrated in Fig. 1A, presenting an analysis of bulk RNA-Seq data from the Human Protein Atlas [35], where CG genes (*MAGEA1*, *MAGEC2,* and *CT83*) show exclusive expression in testis, and SE genes (*FAM83A*, *DSG3,* and *SERPINB5*) in tissues comprising a stratified epithelium (esophagus, vagina, cervix, and skin). Notably, the analysis detected no mRNA of CG and SE genes in lung tissues. This was in striking contrast with mRNAs of *NAPSA*, a lung-specific gene used as control (Fig. 1A). To assess the expression of CG and SE genes with more precision, we analyzed lung transcriptomic data at single-cell resolution, hypothesizing that the genes may be expressed within a discrete cell population. Examining scRNA-Seq data of the LungMap with the ShinyCell web tool [38, 40, 41], we found that *FAM83A* and other SE genes, but not CG genes, exhibited mRNA expression in a small subpopulation of epithelial cells (Fig. 1B and supplementary Fig. S1). The fraction of epithelial lung cells scoring positive for the expression of *FAM83A* and other SE genes was evaluated by analyzing LungMap scRNA-Seq data through the CellxGene platform [42]. This fraction was found to represent 1% for *FAM83A*, and between 0.01% and 7.5% for other SE genes (Fig. 1C). As expected, the fraction of epithelial cells positive for the expression of CG genes was 0%, whereas that for control lung marker genes *NAPSA* and *SFTPC* was 47% and 55%, respectively.

3.2 *FAM83A* and other SE genes are predominantly expressed in airway cell subtypes

We sought to further determine the specific subtypes of epithelial lung cells expressing *FAM83A* and other SE genes. Cell number statistics derived from LungMap scRNA-Seq data indicated that basal/suprabasal lung cells, which reside in airway epithelia, represented the predominant site of *FAM83A* and other SE gene expression (Fig. 2A). *FAM83A* mRNA was also detected in goblet cells, a cell type representing a further stage of differentiation in the airway epithelium [43]. Basal/suprabasal cells have been reported to be more abundant in upper airways and bronchi than in the distal lung [44]. Consistently, analysis of scRNA-Seq data generated from multiple tissues and available through the Human Protein Atlas revealed a higher level of *FAM83A* mRNA in the

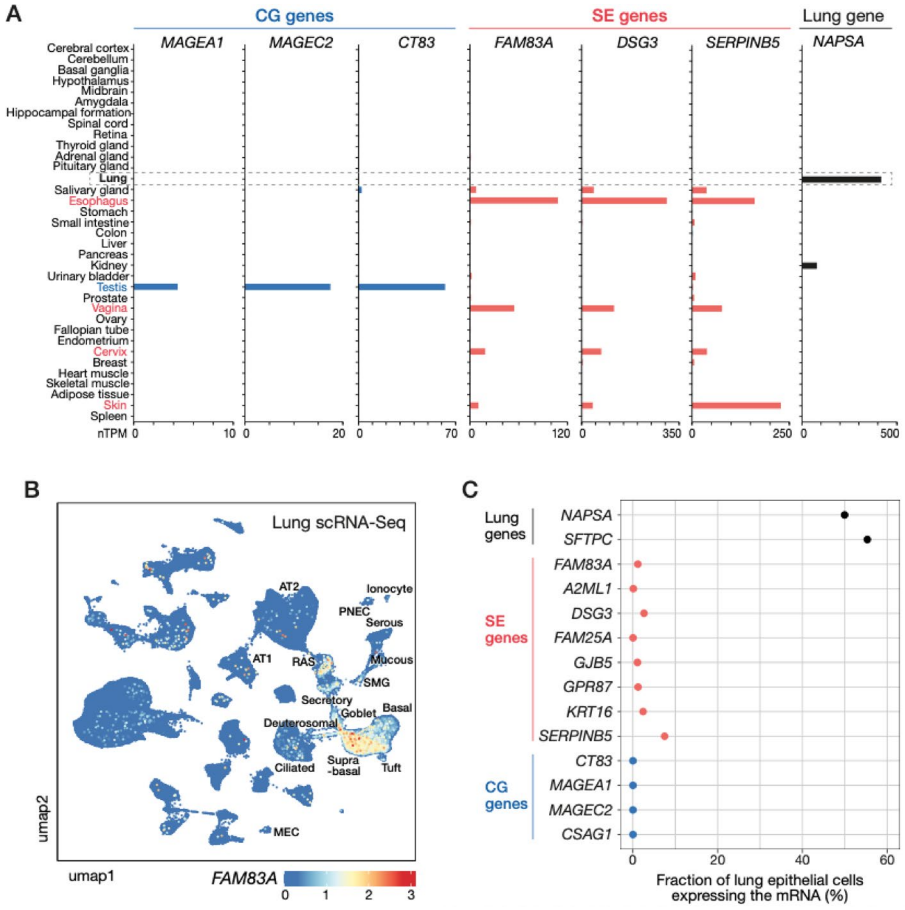

Fig. 1 mRNA of *FAM83A* and other SE genes, but not of CG genes, is detected in a small subpopulation of lung epithelial cells. **A** Bulk RNA-Seq data from the Human Protein Atlas showing expression levels (nTPM) of three cancer-germline (CG) genes (*MAGEA1*, *MAGEC2*, *CT83*), three stratified epithelium (SE) genes (*FAM83A*, *DSG3*, *SERPINB5*), and the lung marker *NAPSA* across 35 normal tissues (y-axis). **B** UMAP representation of scRNA-Seq data from healthy lung tissue, with cells colored according to *FAM83A* expression (Z-scores). Epithelial cell clusters are labeled (see Figure S1 for other cell clusters). **C** Lung scRNA-Seq data were analyzed to evaluate the fraction of lung epithelial cells expressing the indicated genes

bronchus than in the lung (supplementary Fig. S2). Collectively, these findings provided strong evidence that, contrary to *MAGEA1* (and other CG genes), *FAM83A* (like other SE genes) is constitutively expressed in a subpopulation of airway cells whose scarcity in whole lung homogenates precludes detection of *FAM83A* mRNA in bulk tissue analyses.

3.3 Experimental confirmation of *FAM83A* expression in HBEC cells

We next aimed to experimentally confirm the expression of *FAM83A* in airway basal cells. To this end, expression analyses were conducted in ex vivo cultured primary human bronchial epithelial cells (HBEC), which were obtained following digestion and 2D culture expansion of dissected proximal lung airway tissues, as previously described [30]. HBECs that are expanded in these conditions almost exclusively consist of basal cells [45]. Notably, *FAM83A* mRNA expression was detected by RT-qPCR in six out of six independent HBEC cultures, while it remained undetected in bulk lung tissue primarily composed of lung parenchyma (Fig. 2B). Contrastingly, *MAGEA1* mRNA, which could be detected in testis, was completely absent in HBEC cultures. Similar results were obtained with HBEC3-KT (Fig. 2B), a cell line of immortalized primary human bronchial

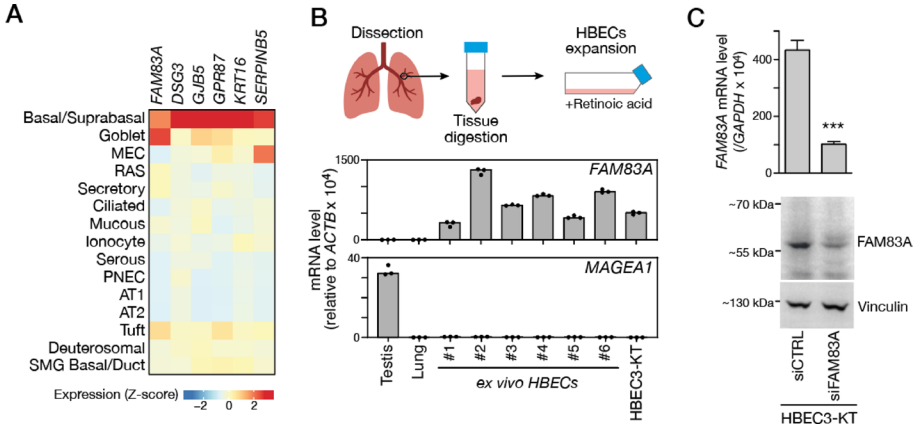

Fig. 2 *FAM83A*, but not *MAGEA1*, is expressed in airway basal epithelial cells. **A** Heatmap showing relative expression levels (Z-scores) of *FAM83A* and five other SE genes across lung epithelial cell subtypes, based on LungMap scRNA-Seq data. **B** Diagram illustrating the procedure for culturing primary HBECs, and results of RT-qPCR analyses for *FAM83A* and *MAGEA1* in testis, lung, ex vivo HBEC cultures, and the HBEC3-KT cell line. Results are the mean of three technical replicates (datapoints). **C** HBEC3-KT cells were transfected with control (siCTRL) or anti-FAM83A (si-FAM83A) siRNAs, and *FAM83A* mRNA and protein levels were evaluated by RT-qPCR and Western blot, respectively. Vinculin served as loading control in the Western blot

epithelial cells exhibiting basal-like characteristics [46]. We further verified FAM83A expression at the protein level in HBEC3-KT cells by performing Western blot analysis. The anti-FAM83A antibody revealed a band migrating slightly above the predicted molecular weight of the protein (47 kDa). This band was specifically reduced in cells where *FAM83A* mRNA was silenced using a siRNA (Fig. 2C), confirming its identity as FAM83A. Together, these results confirmed that *FAM83A* is expressed in airway basal cells at both the mRNA and protein levels, which is not the case for *MAGEA1*.

3.4 Promoter demethylation underlies *FAM83A* activation in HBEC cells

Our previous study in LUAD suggested that *FAM83A* expression is regulated by the DNA methylation status of its promoter [10]. In order to further validate this observation, we first used whole genome bisulfite sequencing (WGBS) data from the Roadmap Epigenomics project [33], and analyzed the methylation status of CpGs contained within a 10 kb region surrounding the transcription start site (TSS) of *FAM83A* in various normal cell types. We observed that CpGs located between positions -1 kb and + 3 kb relative to the *FAM83A* TSS exhibit reduced methylation in skin keratinocytes, which express the gene, and instead maintain high methylation levels in various other cell types where *FAM83A* is repressed (Fig. 3A). Furthermore, by exploring methylation array data of The Cancer Genome Atlas (TCGA) with the Wanderer interactive viewer [34], we were able to show that CpG sites located between positions − 1104 and + 481 relative to the *FAM83A* TSS exhibit significant hypomethylation in LUAD, and that their unmethylated status is correlated with transcriptional upregulation of the gene (Fig. 3B). Together, these observations demonstrate that *FAM83A* promoter DNA methylation is closely associated with its transcriptional activity. Because *FAM83A* is expressed in HBECs, we sought to find out if CpGs within its 5' region are constitutively unmethylated in these cells. To this end, we performed bisulfite sequencing focusing on the *FAM83A* DNA sequence comprising CpGs located between − 97 and + 269 (Fig. 3C). Interestingly, the results showed that CpGs within this region of *FAM83A* are mainly

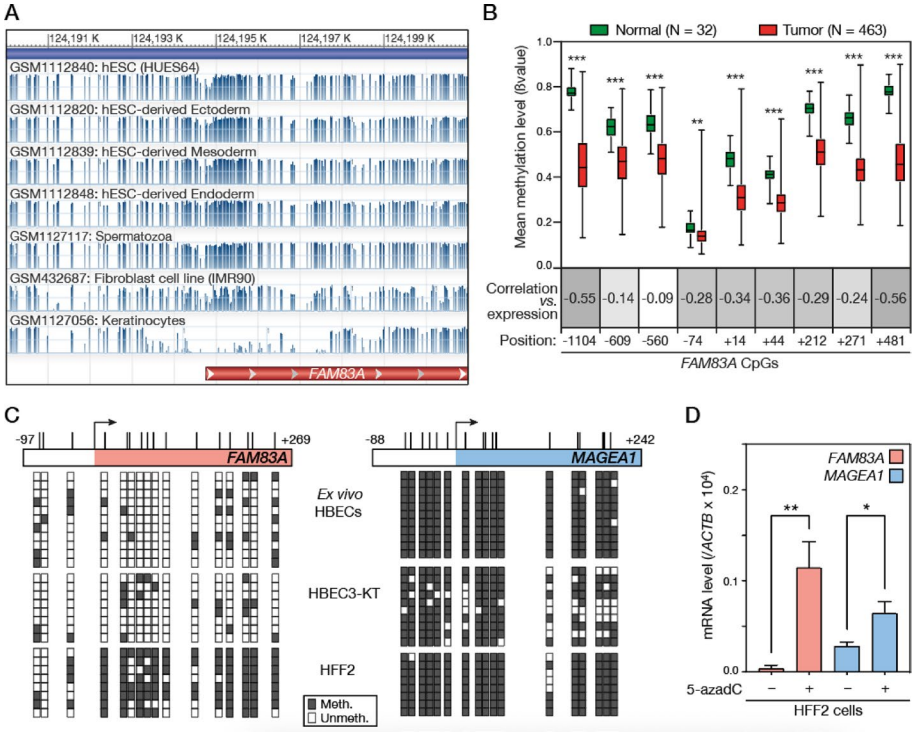

Fig. 3 DNA methylation of the *FAM83A* promoter across cell types and its impact on expression. **A** WGBS data from the Roadmap Epigenomics project, showing the methylation level of CpGs surrounding the *FAM83A* TSS in hESC, hESC induced to differentiate into the three germinal layers, spermatozoa, IMR90 fibroblasts, and keratinocytes. Each vertical line represents the methylation level of one CpG. **B** The Wanderer web-based tool was used to compare methylation levels (ß-value) of indicated CpGs (position relative to the *FAM83A* TSS) in normal lung and LUAD tissues (t-tests; ***: $p \leq 0.001$, **: $p \leq 0.01$;). Correlations between *FAM83A* expression and the CpG methylation level are indicated (Pearson coefficient). **C** Clonal bisulfite-sequencing of the *FAM83A* and *MAGEA1* promoter in ex vivo HBECs, HBEC3-KT and HFF2 cells. Vertical bars indicate the location of CpGs, and the broken arrow indicates the TSS. Open and filled squares represent unmethylated and methylated CpG sites, respectively. Each row corresponds to a single clone. **D** RT-qPCR analysis for *FAM83A* and *MAGEA1* in HFF2 cells that were untreated (–) or treated with 5-azadeoxycytidine (+) (t-tests; **: $p \leq 0.01$, *: $p \leq 0.05$)

unmethylated in ex vivo HBECs and HBEC3-KT cells, and instead highly methylated in cultured human lung fibroblasts (HFF2) where the gene is silent. Of note, many of the CpGs in this same region of *FAM83A* were methylated in AT2 cells (supplementary Fig. S3), according to WGBS data [47]. In striking contrast, CpGs within the *MAGEA1* promoter were mostly methylated in ex vivo HBECs and HBEC3KT, as well as in HFF2 (Fig. 3C). Finally, in order to provide an experimental demonstration that *FAM83A* expression depends on DNA demethylation, we exposed HFF2 cells to 5-azadeoxycytidine (5-azadC), a DNA methylation inhibitor, and evaluated the expression of *FAM83A* after 3 days by RT-qPCR. Treatment with 5-azadC resulted in marked induction of *FAM83A* (Fig. 3D), which was not only comparable to, but even slightly greater than, that observed for *MAGEA1*, a well-established DNA methylation-sensitive gene [48]. Collectively, these results indicate that *FAM83A* expression is regulated by DNA methylation, and that its expression in HBECs is associated with the unmethylated status of its promoter in these cells.

3.5 *FAM83A*-overexpressing LUAD cells express basal/suprabasal and goblet cell markers

Our results indicate that *FAM83A* belongs to a gene expression program that characterizes airway basal/suprabasal cells and cells transiting towards goblet cell differentiation.

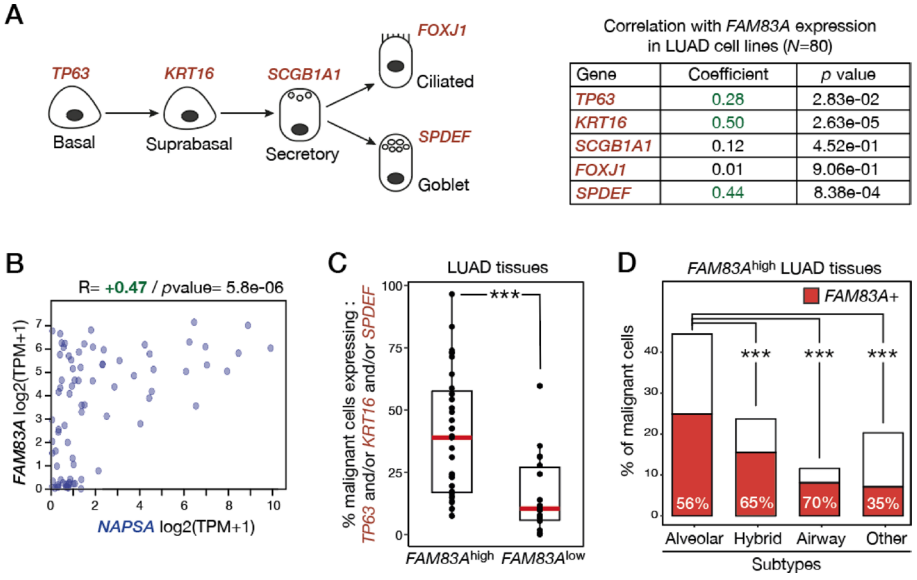

Fig. 4 *FAM83A* expression in LUAD coexists with AT2 marker *NAPSA*, and correlates with that of airway cell markers. **A** Indicated markers of lung airway cell subtypes were tested for their expression correlation scores (Spearman coefficient) with *FAM83A* in LUAD cell lines (CCLE), using the Depmap Portal. **B** Scatter plot showing co-expression of *FAM83A* and AT2-cell marker *NAPSA* in LUAD cell lines of the CCLE. **C** scRNA-Seq data of LUAD tissues were analyzed, and tumor samples were divided into *FAM83A*^{high} (≥ 30% malignant cells expressing *FAM83A*) and *FAM83A*^{low} (< 10% malignant cells expressing *FAM83A*) (t-tests; ***: $p \leq 0.001$). Boxplots represent the proportion of cells expressing at least one of the indicated markers in the different samples. **D** Malignant cells belonging to *FAM83A*^{high} LUAD samples were classified into different subtypes (alveolar, hybrid, airway, other) according to the expression of specific markers (see text), and the proportion of cells expressing *FAM83A* was measured in each cell subtype (Chi-square test; ***: $p \leq 0.001$)

This observation suggested that *FAM83A* expression in LUAD might reflect a shift of alveolar AT2 cells (the cell of origin) towards an airway differentiation program during tumor progression. To evaluate this hypothesis, we assessed whether expression of *FAM83A* in LUAD correlates with that of markers defining the basal-to-goblet cell differentiation axis. Previously established lung epithelial subtype marker genes (*TP63*, *KRT16*, *SCGB1A1*, *FOXJ1*, *SPDEF*) were selected [49–51], and their cell type-specific expression was verified in lung scRNA-Seq data (Fig. 4A, supplementary Fig. S4). Interestingly, one of these markers (*KRT16*) belonged to the SE cluster of genes we identified previously [10]. We then interrogated transcriptomic data of the Cancer Cell Line Encyclopedia (CCLE) with the Depmap web interface [37, 52], in order to determine pairwise correlation coefficients between the expression of *FAM83A* and each differentiation marker in LUAD cell lines (Fig. 4A). Consistent with our hypothesis, *FAM83A* expression in LUAD cell lines displayed positive association with markers of basal, suprabasal and goblet cells (*TP63*, *KRT16*, and *SPDEF*, respectively). We then examined the mRNA expression of *NAPSA*, a marker of AT2 cells often used to diagnose LUAD [53, 54]. A majority (74%) of LUAD cell lines ($N = 80$) scored positive for *NAPSA* expression ($\log2(\text{TPM} + 1) \geq 0.5$), and among these 78% also scored positive for *FAM83A* expression (Fig. 4B). These results support the idea that LUAD tumors often comprise AT2 cells in which *FAM83A* became activated, a process associated with the acquisition of basal, suprabasal, and goblet cell features. To further address this possibility, we examined scRNA-Seq data of LUAD tissue samples [55], focusing on the malignant cell population. Our aim was to determine if the association of *FAM83A* expression with AT2 and basal/

suprabasal/goblet markers also pertains in vivo. We first separated LUAD samples into *FAM83A*^{high} tumors (≥ 30% malignant cells expressing *FAM83A*, $N = 35$) and *FAM83A*^{low} tumors (< 10% malignant cells expressing *FAM83A*, $N = 18$), and evaluated the proportion of malignant cells within these two groups of tumors that express at least one of the airway basal/suprabasal/globlet markers (*TP63*, *KRT16*, and *SPDEF*). The results showed that the *FAM83A*^{high} LUAD samples contained a higher proportion of malignant cells expressing these airway markers (Fig. 4C). To investigate cellular-level correlations, we divided malignant cells from *FAM83A*^{high} tumors into four groups: those expressing only the AT2 marker *NAPSA* ("alveolar" cells), those expressing both *NAPSA* and at least one of the three airway markers ("hybrid" cells), those expressing at least one of the three airway markers but not *NAPSA* ("airway" cells), and those lacking all markers ("other" cells; Fig. 4D). The results indicate that although *FAM83A* is expressed in a substantial proportion (56%) of alveolar malignant cells, its expression is more prevalent in hybrid (65%) and airway (70%) malignant cells (Fig. 4D). This pattern therefore supports the association between *FAM83A* expression and the shift of alveolar cells toward airway differentiation.

Finally, we also compared the expression of *FAM83A* with that of *MAGEA1* in LUAD cell lines and tissues, and found no correlation (supplementary Fig. S5), thereby indicating that up-regulation of these two genes in LUAD does not rely on a common mechanism of de-repression.

4 Discussion

FAM83A, a gene mainly active in tissues comprising a stratified epithelium (esophagus, skin, vagina), has been reported to be overexpressed in a variety of malignancies and to correlate with poor clinical outcomes [11]. Although its cellular function still needs to be fully elucidated, a number of studies show that the FAM83A protein exerts pro-tumoral functions by modulating molecular pathways involved in cell proliferation and differentiation [56]. Recent work from our laboratory demonstrated that in LUAD, *FAM83A* overexpression is linked to DNA hypomethylation of its promoter, implicating epigenetic mechanisms in its upregulation in tumor cells [10]. Loss of DNA methylation is well known to contribute to aberrant gene activation in tumors, with the germline-specific gene *MAGEA1* representing a prototypical example of a gene abnormally activated by this epigenetic alteration [57]. However, the mechanisms underlying DNA hypomethylation in tumors remain largely unresolved. In this study, we show that while *MAGEA1* activation in LUAD arises from an aberrant process of DNA demethylation, *FAM83A* demethylation and upregulation appears to reflect epigenetic reprogramming of the cell of origin toward an alternative lung epithelial differentiation trajectory.

By examining scRNA-Seq data of normal lung, we found that *FAM83A* is expressed in a defined subset of airway epithelial cells corresponding to basal/suprabasal and goblet populations. Whether FAM83A protein expression recapitulates this cell-type specificity could not be demonstrated, as immunofluorescence is currently precluded by the lack of suitable anti-FAM83A antibodies. The absence of secretory cells within the cluster of *FAM83A*-defined cells is intriguing, as secretory cells are classically considered an intermediate state between basal/suprabasal and goblet differentiation [58]. A recent study, however, has demonstrated the existence of hybrid airway cells expressing markers of both basal and goblet cells, in particular in condition of lung injury and regeneration

[59]. While the *FAM83A* expression pattern we describe may be consistent with specific epithelial cell states or transitions, our data are limited to steady-state conditions and do not allow us to infer a role in differentiation, injury response, or regeneration. Accordingly, any link between *FAM83A* expression and these processes remains speculative and will require dedicated functional studies. Importantly, the present study was designed to investigate the epigenetic mechanisms underlying *FAM83A* activation in LUAD rather than the mechanistic contribution of this gene to airway epithelial differentiation, which remains to be clarified in future work.

Current evidence suggests that LUAD primarily arises from alveolar AT2 cells [27, 28, 60]. Surprisingly, our study revealed that a number of LUAD samples comprise *FAM83A*-expressing malignant cells that display characteristics of airway lineages. Importantly, we identified tumor cell populations that concomitantly express a canonical AT2 marker (*NAPSA*) together with *FAM83A* and airway lineage (basal/suprabasal/goblet) markers, indicating the presence of hybrid epithelial states within the tumor. These findings align with previous reports describing a high plasticity of malignant cells in LUAD, and the appearance of "AT2-like" cells undergoing transdifferentiation toward airway regenerative epithelial states [60–62]. Together, our data suggest that *FAM83A* demethylation and activation in LUAD is an integral component of the reprogramming of AT2 cells toward airway epithelial identities. Moreover, the association of high *FAM83A* expression with reduced survival of LUAD patients implies that this reprogramming may impact tumor aggressiveness. It remains unclear whether the redirection of AT2 cells toward alveolar states occurs during tumorigenesis or instead pre-exists within a subset of normal lung epithelial cells. The latter possibility appears unlikely, as cells co-expressing *NAPSA*, *FAM83A*, and basal, suprabasal, or goblet markers were scarcely detected (0.0015% of epithelial cells) in scRNA-Seq data from normal lung tissue.

FAM83A overexpression has been reported in several tumor types beyond LUAD, notably in breast (BRCA) and pancreatic (PAAD) cancers, where elevated expression of the gene also correlates with poorer patient survival [63, 64]. Interestingly, visualization of single-cell RNA sequencing data on the Human Protein Atlas (HPA) platform reveals that *FAM83A* is expressed in discrete subsets of epithelial cells within healthy breast and pancreatic tissues (supplementary Fig. S6) [65]. This observation raises the possibility that upregulation of *FAM83A* in BRCA and PAAD might also reflect reprogramming of tumor cells toward regenerative epithelial states in the corresponding tissues.

Careful examination of scRNA-Seq of normal lung revealed no expression of *MAGEA1* and other CG genes in any cell type. Furthermore, we showed that the expression of *MAGEA1* and other CG genes in tumors does not correlate with that of *FAM83A* and other SE genes. It is therefore very likely that hypomethylation of *MAGEA1* and *FAM83A* in LUAD are driven by distinct processes. Thus, whereas *MAGEA1* de-repression in lung tumor cells represents an aberrant event resulting from a global process of DNA methylation loss [19, 57, 66, 67], *FAM83A* promoter demethylation seem to occur as part of an intrinsic program of airway basal-to-goblet differentiation. More broadly, we conclude that activation of CG genes in tumor cells results from *epigenetic dysregulation* leading to the aberrant de-repression of spermatogenic genes, while activation of SE genes entails *epigenetic reprogramming* redirecting tumor cells toward an existing airway epithelial differentiation trajectory.

Our observations identify DNA methylation as a key mechanism controlling the cell type-specific expression of *FAM83A*, and in particular in determining whether the gene is active or repressed in specific subtypes of lung epithelial cells. This is a significant finding, as only a few genes rely mainly on DNA methylation to enforce cell type-specific expression [68]. It will be important to investigate how *FAM83A* methylation patterns evolve during airway lineage specification. Given that several transcription factors potentially involved in this regulatory process have been identified [69], future studies should assess whether these factors contribute to changes in the *FAM83A* promoter methylation and thereby modulate its expression across airway and alveolar cell types.

Supplementary Information

The online version contains supplementary material available at https://doi.org/10.1007/s12672-026-05380-8.

Supplementary Material 1.

Supplementary Material 2.

Author contributions

C.W. and C.D.S. designed the study; C.W. conducted bioinformatics analyses; C.W., F.M.C., and M.L. performed experiments; C.D.S., F.M.C, and C.P. supervised the project; All authors reviewed the manuscript.

Funding

This work is supported by grants from the D.G. Higher Education and Scientific Research of the Fédération Wallonie-Bruxelles (Action de Recherche Concertées, ARC 24/29-142) and from the Fondation Louvain (Legs Heyens). F.M.C. is a recipient of a grant from FRS-FNRS, Belgium (SPD 40017491).

Data availability

All datasets analyzed in this study are available from public repositories, and include: GTEx v8 RNA-Seq datasets (https://www.gtexportal.org/home/downloads/adult-gtex/bulk_tissue_expression) and scRNA-Seq datasets (https://www.proteinatlas.org/humanproteome/single+cell/single+cell+type/data#datasets) through the Human Protein Atlas portal (https://www.proteinatlas.org), scRNA-Seq data of the LungMap ShinyCell (https://app.lungmap.net/app/shinycell-human-lung-cellref, dataset ID: LMEX0000004396), WGBS data from the Roadmap Epigenomics project (https://www.ncbi.nlm.nih.gov/geo/roadmap/epigenomics, GEO datasets: GSM1112840, GSM1112820, GSM1112839, GSM1112848, GSM1127117, GSM432687, GSM1127056), LUAD-TCGA methylation arrays through the TCGA Wanderer (http://maplab.imppc.org/wanderer/, https://portal.gdc.cancer.gov/projects/TCGA-LUAD), RNA-Seq data of the CCLE through the Depmap explorer tool (https://depmap.org/portal/data_explorer_2/, SRA accession number PRJNA523380), CellxGene LUAD single-cell datasets (https://cellxgene.cziscience.com/collections/edb893ee-4066-4128-9aec-5eb2b03f8287), and LUAD-TCGA RNA-Seq datasets through GEPIA2 correlation analysis tool (http://gepia2.cancer-pku.cn/#correlation, https://portal.gdc.cancer.gov/projects/TCGA-LUAD).

Declarations

Ethics approval and consent to participate

Not applicable.

Consent for publication

Not applicable.

Competing interests

The authors declare no competing interests.

Received: 4 March 2026 / Accepted: 3 June 2026

Published online: 07 June 2026

References

1. Bird A. DNA methylation patterns and epigenetic memory. Genes Dev. 2002;16(1):6–21.
2. Lokk K, Modhukur V, Rajashekar B, Martens K, Magi R, Kolde R, et al. DNA methylome profiling of human tissues identifies global and tissue-specific methylation patterns. Genome Biol. 2014;15(4):r54. https://doi.org/10.1186/gb-2014-15-4-r54.
3. Loyfer N, Magenheim J, Peretz A, Cann G, Bredno J, Klochendler A, et al. A DNA methylation atlas of normal human cell types. Nature. 2023;613(7943):355–64. https://doi.org/10.1038/s41586-022-05580-6.
4. Bocklandt S, Lin W, Sehl ME, Sanchez FJ, Sinsheimer JS, Horvath S, et al. Epigenetic predictor of age. PLoS ONE. 2011;6(6):e14821. https://doi.org/10.1371/journal.pone.0014821.
5. Ushijima T, Watanabe N, Okochi E, Kaneda A, Sugimura T, Miyamoto K. Fidelity of the methylation pattern and its variation in the genome. Genome Res. 2003;13(5):868–74.

6. Baylin SB, Jones PA. A decade of exploring the cancer epigenome - biological and translational implications. Nat Rev Cancer. 2011;11(10):726–34. https://doi.org/10.1038/nrc3130.
7. Esteller M. Epigenetics in cancer. N Engl J Med. 2008;358(11):1148–59.
8. Van Tongelen A, Loriot A, De Smet C. Oncogenic roles of DNA hypomethylation through the activation of cancer-germline genes. Cancer Lett. 2017;396:130–7. https://doi.org/10.1016/j.canlet.2017.03.029.
9. De Smet C, Loriot A. DNA hypomethylation and activation of germline-specific genes in cancer. Adv Exp Med Biol. 2013;754:149–66.
10. Diacofotaki A, Loriot A, De Smet C. Identification of Tissue-Specific Gene Clusters Induced by DNA Demethylation in Lung Adenocarcinoma: more Than Germline Genes. Cancers (Basel). 2022;14(4):1007. https://doi.org/10.3390/cancers14041007.
11. Bartel CA, Parameswaran N, Cipriano R, Jackson MW. FAM83 proteins: fostering new interactions to drive oncogenic signaling and therapeutic resistance. Oncotarget. 2016;7(32):52597–612. https://doi.org/10.18632/oncotarget.9544.
12. Lee SY, Meier R, Furuta S, Lenburg ME, Kenny PA, Xu R, et al. FAM83A confers EGFR-TKI resistance in breast cancer cells and in mice. J Clin Invest. 2012;122(9):3211–20. https://doi.org/10.1172/JCI60498.
13. Marino N, German R, Podicheti R, Rockey P, Sandusky GE, Temm CJ, et al. FAM83A is a potential biomarker for breast cancer initiation. Biomark Res. 2022;10(1):8. https://doi.org/10.1186/s40364-022-00353-9.
14. Yuan Y, Hao L, Huang JS, Zhao FY, Ju YH, Wang JM, et al. Promotion of stem cell-like phenotype of lung adenocarcinoma by FAM83A via stabilization of ErbB2. Cell Death Dis. 2024;15(6):460. https://doi.org/10.1038/s41419-024-06853-w.
15. Cipriano R, Miskimen KL, Bryson BL, Foy CR, Bartel CA, Jackson MW. Conserved oncogenic behavior of the FAM83 family regulates MAPK signaling in human cancer. Mol Cancer Res. 2014;12(8):1156–65. https://doi.org/10.1158/1541-7786.MCR-13-0289.
16. Liu C, Peng X, Li Y, Liu S, Hou R, Zhang Y, et al. Positive feedback loop of FAM83A/PI3K/AKT/c-Jun induces migration, invasion and metastasis in hepatocellular carcinoma. Biomed Pharmacother. 2020;123:109780. https://doi.org/10.1016/j.biopha.2019.109780.
17. Zheng YW, Li ZH, Lei L, Liu CC, Wang Z, Fei LR, et al. FAM83A Promotes Lung Cancer Progression by Regulating the Wnt and Hippo Signaling Pathways and Indicates Poor Prognosis. Front Oncol. 2020;10:180. https://doi.org/10.3389/fonc.2020.00180.
18. Abdel-Fatah TM, McArdle SE, Johnson C, Moseley PM, Ball GR, Pockley AG, et al. HAGE (DDX43) is a biomarker for poor prognosis and a predictor of chemotherapy response in breast cancer. Br J Cancer. 2014;110(10):2450–61. https://doi.org/10.1038/bjc.2014.168.
19. Cannuyer J, Van Tongelen A, Loriot A, De Smet C. A gene expression signature identifying transient DNMT1 depletion as a causal factor of cancer-germline gene activation in melanoma. Clin Epigenetics. 2015;7:114. https://doi.org/10.1186/s13148-015-0147-4.
20. Hervouet E, Lalier L, Debien E, Cheray M, Geairon A, Rogniaux H, et al. Disruption of Dnmt1/PCNA/UHRF1 interactions promotes tumorigenesis from human and mice glial cells. PLoS ONE. 2010;5(6):e11333. https://doi.org/10.1371/journal.pone.0011333.
21. Jia Y, Li P, Fang L, Zhu H, Xu L, Cheng H, et al. Negative regulation of DNMT3A de novo DNA methylation by frequently overexpressed UHRF family proteins as a mechanism for widespread DNA hypomethylation in cancer. Cell Discov. 2016;2:16007. https://doi.org/10.1038/celldisc.2016.7.
22. O'Hagan HM, Wang W, Sen S, Destefano Shields C, Lee SS, Zhang YW, et al. Oxidative damage targets complexes containing DNA methyltransferases, SIRT1, and polycomb members to promoter CpG islands. Cancer Cell. 2011;20(5):606–19. https://doi.org/10.1016/j.ccr.2011.09.012.
23. Russler-Germain DA, Spencer DH, Young MA, Lamprecht TL, Miller CA, Fulton R, et al. The R882H DNMT3A mutation associated with AML dominantly inhibits wild-type DNMT3A by blocking its ability to form active tetramers. Cancer Cell. 2014;25(4):442–54. https://doi.org/10.1016/j.ccr.2014.02.010.
24. Davies A, Zoubeidi A, Beltran H, Selth LA. The transcriptional and epigenetic landscape of cancer cell lineage plasticity. Cancer Discov. 2023;13(8):1771–88. https://doi.org/10.1158/2159-8290.CD-23-0225.
25. Scaffidi P, Misteli T. Cancer epigenetics: from disruption of differentiation programs to the emergence of cancer stem cells. Cold Spring Harb Symp Quant Biol. 2010;75:251–8. https://doi.org/10.1101/sqb.2010.75.007.
26. Ehrlich M. DNA hypomethylation in cancer cells. Epigenomics. 2009;1(2):239–59.
27. Blanpain C. Tracing the cellular origin of cancer. Nat Cell Biol. 2013;15(2):126–34. https://doi.org/10.1038/ncb2657.
28. Mainardi S, Mijimolle N, Francoz S, Vicente-Duenas C, Sanchez-Garcia I, Barbacid M. Identification of cancer initiating cells in K-Ras driven lung adenocarcinoma. Proc Natl Acad Sci USA. 2014;111(1):255–60. https://doi.org/10.1073/pnas.1320383110.
29. Shi M, Mear L, Karlsson M, Alvez MB, Digre A, Schutten R, et al. A resource for whole-body gene expression map of human tissues based on integration of single cell and bulk transcriptomics. Genome Biol. 2025;26(1):152. https://doi.org/10.1186/s13059-025-03616-4.
30. Carlier FM, Dupasquier S, Ambroise J, Detry B, Lecocq M, Bietry-Claudet C, et al. Canonical WNT pathway is activated in the airway epithelium in chronic obstructive pulmonary disease. EBioMedicine. 2020;61:103034. https://doi.org/10.1016/j.ebiom.2020.103034.
31. Tilman G, Arnoult N, Lenglez S, Van Beneden A, Loriot A, De Smet C, et al. Cancer-linked satellite 2 DNA hypomethylation does not regulate Sat2 non-coding RNA expression and is initiated by heat shock pathway activation. Epigenetics. 2012;7(8):903–13. https://doi.org/10.4161/epi.21107.
32. De Smet C, Loriot A, Boon T. Promoter-dependent mechanism leading to selective hypomethylation within the 5' region of gene MAGE-A1 in tumor cells. Mol Cell Biol. 2004;24(11):4781–90.
33. Roadmap Epigenomics C, Kundaje A, Meuleman W, Ernst J, Bilenky M, Yen A, et al. Integrative analysis of 111 reference human epigenomes. Nature. 7539;518(7539):317–30. https://doi.org/10.1038/nature14248.
34. Diez-Villanueva A, Mallona I, Peinado MA. Wanderer, an interactive viewer to explore DNA methylation and gene expression data in human cancer. Epigenetics Chromatin. 2015;8:22. https://doi.org/10.1186/s13072-015-0014-8.
35. Uhlen M, Bjorling E, Agaton C, Szigyarto CA, Amini B, Andersen E, et al. A human protein atlas for normal and cancer tissues based on antibody proteomics. Mol Cell Proteomics. 2005;4(12):1920–32. https://doi.org/10.1074/mcp.M500279-MCP200.

36. Tang Z, Kang B, Li C, Chen T, Zhang Z. GEPIA2: an enhanced web server for large-scale expression profiling and interactive analysis. Nucleic Acids Res. 2019;47:W556–60. https://doi.org/10.1093/nar/gkz430.
37. Arafeh R, Shibue T, Dempster JM, Hahn WC, Vazquez F. The present and future of the Cancer Dependency Map. Nat Rev Cancer. 2025;25(1):59–73. https://doi.org/10.1038/s41568-024-00763-x.
38. Ouyang JF, Kamaraj US, Cao EY, Rackham OJL. ShinyCell: simple and sharable visualization of single-cell gene expression data. Bioinformatics. 2021;37(19):3374–6. https://doi.org/10.1093/bioinformatics/btab209.
39. Salcher S, Sturm G, Horvath L, Untergasser G, Kuempers C, Fotakis G, et al. High-resolution single-cell atlas reveals diversity and plasticity of tissue-resident neutrophils in non-small cell lung cancer. Cancer Cell. 2022;40(12):1503-20 e8. https://doi.org/10.1016/j.ccell.2022.10.008.
40. Ardini-Poleske ME, Clark RF, Ansong C, Carson JP, Corley RA, Deutsch GH, et al. LungMAP: The Molecular Atlas of Lung Development Program. Am J Physiol Lung Cell Mol Physiol. 2017;313(5):L733–40. https://doi.org/10.1152/ajplung.00139.2017.
41. Guo M, Morley MP, Jiang C, Wu Y, Li G, Du Y, et al. Guided construction of single cell reference for human and mouse lung. Nat Commun. 2023;14(1):4566. https://doi.org/10.1038/s41467-023-40173-5.
42. Program CZICS, Abdulla S, Aevermann B, Assis P, Badajoz S, Bell SM, et al. CZ CELLxGENE discover: a single-cell data platform for scalable exploration, analysis and modeling of aggregated data. Nucleic Acids Res. 2025;53:D886–900. https://doi.org/10.1093/nar/gkae1142.
43. Whitsett JA, Kalin TV, Xu Y, Kalinichenko VV. Building and Regenerating the Lung Cell by Cell. Physiol Rev. 2019;99(1):513–54. https://doi.org/10.1152/physrev.00001.2018.
44. Boers JE, Ambergen AW, Thunnissen FB. Number and proliferation of basal and parabasal cells in normal human airway epithelium. Am J Respir Crit Care Med. 1998;157:2000–6. https://doi.org/10.1164/ajrccm.157.6.9707011.
45. Hajj R, Baranek T, Le Naour R, Lesimple P, Puchelle E, Coraux C. Basal cells of the human adult airway surface epithelium retain transit-amplifying cell properties. Stem Cells. 2007;25(1):139–48. https://doi.org/10.1634/stemcells.2006-0288.
46. Ramirez RD, Sheridan S, Girard L, Sato M, Kim Y, Pollack J, et al. Immortalization of human bronchial epithelial cells in the absence of viral oncoproteins. Cancer Res. 2004;64(24):9027–34. https://doi.org/10.1158/0008-5472.CAN-04-3703.
47. Zuber V, Marconett CN, Shi J, Hua X, Wheeler W, Yang C, et al. Pleiotropic analysis of lung cancer and blood triglycerides. J Natl Cancer Inst. 2016. https://doi.org/10.1093/jnci/djw167.
48. Cannuyer J, Loriot A, Parvizi GK, De Smet C. Epigenetic hierarchy within the MAGEA1 cancer-germline gene: promoter DNA methylation dictates local histone modification. PLoS ONE. 2013;8(3):e58743.
49. Chen G, Korfhagen TR, Xu Y, Kitzmiller J, Wert SE, Maeda Y, et al. SPDEF is required for mouse pulmonary goblet cell differentiation and regulates a network of genes associated with mucus production. J Clin Invest. 2009;119(10):2914–24. https://doi.org/10.1172/JCI39731.
50. Ruiz Garcia S, Deprez M, Lebrigand K, Cavard A, Paquet A, Arguel MJ, et al. Novel dynamics of human mucociliary differentiation revealed by single-cell RNA sequencing of nasal epithelial cultures. Development. 2019. https://doi.org/10.1242/dev.177428.
51. Sun X, Perl AK, Li R, Bell SM, Sajti E, Kalinichenko VV, et al. A census of the lung: CELLCARDS from LungMAP. Dev Cell. 2022;57(1):112-45 e2. https://doi.org/10.1016/j.devcel.2021.11.007.
52. Cancer Cell Line Encyclopedia C, Genomics of Drug Sensitivity in Cancer C. Pharmacogenomic agreement between two cancer cell line data sets. Nature. 2015;528(7580):84–7. https://doi.org/10.1038/nature15736.
53. Hirano T, Auer G, Maeda M, Hagiwara Y, Okada S, Ohira T, et al. Human tissue distribution of TA02, which is homologous with a new type of aspartic proteinase, napsin A. Jpn J Cancer Res. 2000;91(10):1015–21. https://doi.org/10.1111/j.1349-7006.2000.tb00879.x.
54. Lee JG, Kim S, Shim HS. Napsin A is an independent prognostic factor in surgically resected adenocarcinoma of the lung. Lung Cancer. 2012;77(1):156–61. https://doi.org/10.1016/j.lungcan.2012.02.013.
55. Sikkema L, Ramirez-Suastegui C, Strobl DC, Gillett TE, Zappia L, Madissoon E, et al. An integrated cell atlas of the lung in health and disease. Nat Med. 2023;29(6):1563–77. https://doi.org/10.1038/s41591-023-02327-2.
56. Jiang Y, Yu J, Zhu T, Bu J, Hu Y, Liu Y, et al. Involvement of FAM83 Family Proteins in the Development of Solid Tumors: an Update Review. J Cancer. 2023;14(10):1888–903. https://doi.org/10.7150/jca.83420.
57. De Smet C, De Backer O, Faraoni I, Lurquin C, Brasseur F, Boon T. The activation of human gene MAGE-1 in tumor cells is correlated with genome-wide demethylation. Proc Natl Acad Sci USA. 1996;93(14):7149–53.
58. Ruysseveldt E, Martens K, Steelant B. Airway Basal Cells, Protectors of Epithelial Walls in Health and Respiratory Diseases. Frontiers in Allergy. 2021;2:787128. https://doi.org/10.3389/falgy.2021.787128.
59. Martins LR, Sieverling L, Michelhans M, Schiller C, Erkut C, Grunewald TGP, et al. Single-cell division tracing and transcriptomics reveal cell types and differentiation paths in the regenerating lung. Nat Commun. 2024;15(1):2246. https://doi.org/10.1038/s41467-024-46469-4.
60. Wang Z, Li Z, Zhou K, Wang C, Jiang L, Zhang L, et al. Deciphering cell lineage specification of human lung adenocarcinoma with single-cell RNA sequencing. Nature Commun. 2021;12(1):6500. https://doi.org/10.1038/s41467-021-26770-2.
61. Laughney AM, Hu J, Campbell NR, Bakhoum SF, Setty M, Lavallee VP, et al. Regenerative lineages and immune-mediated pruning in lung cancer metastasis. Nat Med. 2020;26(2):259–69. https://doi.org/10.1038/s41591-019-0750-6.
62. Marjanovic ND, Hofree M, Chan JE, Canner D, Wu K, Trakala M, et al. Emergence of a high-plasticity cell state during lung cancer evolution. Cancer Cell. 2020;38(2):229-46 e13. https://doi.org/10.1016/j.ccell.2020.06.012.
63. Jin Y, Yu J, Jiang Y, Bu J, Zhu T, Gu X, et al. Comprehensive analysis of the expression, prognostic significance, and function of FAM83 family members in breast cancer. World J Surg Oncol. 2022;20(1):172. https://doi.org/10.1186/s12957-022-02636-9.
64. Zou W, Wang H, Wu D, Wu Y, Zhou K, Lian Y, et al. ncRNA-mediated upregulation of FAM83A is associated with poor prognosis and immune infiltration in pancreatic cancer. Front Endocrinol (Lausanne). 2023;14:1093042. https://doi.org/10.3389/fendo.2023.1093042.
65. Karlsson M, Zhang C, Mear L, Zhong W, Digre A, Katona B, et al. A single-cell type transcriptomics map of human tissues. Sci Adv. 2021. https://doi.org/10.1126/sciadv.abh2169.
66. Cadieux B, Ching TT, VandenBerg SR, Costello JF. Genome-wide hypomethylation in human glioblastomas associated with specific copy number alteration, methylenetetrahydrofolate reductase allele status, and increased proliferation. Cancer Res. 2006;66(17):8469–76.

67. Woloszynska-Read A, Mhawech-Fauceglia P, Yu J, Odunsi K, Karpf AR. Intertumor and intratumor NY-ESO-1 expression heterogeneity is associated with promoter-specific and global DNA methylation status in ovarian cancer. Clin Cancer Res. 2008;14(11):3283–90.
68. Bestor TH, Edwards JR, Boulard M. Notes on the role of dynamic DNA methylation in mammalian development. Proc Natl Acad Sci USA. 2015;112(22):6796–9. https://doi.org/10.1073/pnas.1415301111.
69. Maeda Y, Dave V, Whitsett JA. Transcriptional control of lung morphogenesis. Physiol Rev. 2007;87(1):219–44. https://doi.org/10.1152/physrev.00028.2006.

Publisher's Note